

Galactic halos of self-interacting dark matter

Steen Hannestad

Institute of Physics and Astronomy, University of Aarhus, DK-8000 Århus C, Denmark

(October 7, 2018)

Recent, very accurate simulations of galaxy formation have revealed that the standard cold dark matter model has great difficulty in explaining the detailed structure of galaxies. One of the major problems is that galactic halos are too centrally concentrated. Dark matter self-interactions have been proposed as a possible means of resolving this inconsistency. Here, we investigate quantitatively the effect of dark matter self interactions on formation of galactic halos. Our numerical framework is extremely simple, while still keeping the essential physics. We confirm that strongly self-interacting dark matter leads to less centrally concentrated structures. Interestingly, we find that for a range of different interaction strengths, the dark matter halos are unstable to particle ejection on a timescale comparable to the Hubble time.

PACS numbers: 95.35.+d, 98.62.Gq, 14.80.-j

I. INTRODUCTION

The concept of dark matter was originally introduced by Zwicky in 1933 [1]. to explain the behaviour of individual galaxy clusters. Since then the dark matter has been determined to be essential for explaining a vast number of astronomical observations. The cold dark matter model has, with modifications, been very successful in explaining how structure forms in the universe [2]. However, it was recently realised that the CDM model is apparently unable to explain the dynamics of individual galaxies. Very high resolution simulations have shown that there should be much more sub-structure in the halos of typical galaxies than is observed. Numerical simulations predict that the local group should at present contain about 1000 distinct dark matter halos. Observations yield a number which is a factor of ten lower [3,4]. Also, lensing measurements of clusters seem to indicate a constant density core, in strong contrast with numerical simulations [4,5]. Also, the central density profile in galactic halos is predicted to be much steeper than in real galaxies [6–10]. However, this is not a completely settled issue. For instance Kravtsov *et al.* [11] find that CDM simulations are consistent with observations.

If the problem with CDM halos persists, then it could possibly be remedied if structure formation is somehow suppressed on small scales. One such possibility is that perhaps the dark matter is not cold, but rather “warm”, i.e. dark matter particles have masses around 1 keV and therefore have significant thermal motion around the time of matter-radiation decoupling [12]. That would suppress structure formation on galactic scales and below. However, warm dark matter may have problems in describing properly the properties of clusters. Another possibility is that the initial power spectrum has a cut-off at some wavelength, corresponding to the substructures in galaxies [13], so that no structure below this scale will grow initially.

A quite different possibility is that the discrepancy has

to do with the interaction properties of the dark matter, not just the mass of the individual particles. It was recently proposed by Spergel and Steinhardt [14], that dark matter with strong self-interactions could make the cold dark matter model consistent with observations. Strongly self-interacting dark matter will tend to produce halos with shallower core density profiles, thereby alleviating the problem of the central mass concentration. Although the simple arguments provided in Ref. [14] are quite convincing, it seems very important to test the implications of self interacting dark matter on a more quantitative basis. That is the purpose of the present paper. With the help of a very simple numerical scheme, we solve the Boltzmann equation describing the phase-space evolution of collisional dark matter and are thus able to calculate final state density and velocity distributions.

Intriguingly, we find that there is a range of parameters for which there exist no stable equilibria, even on a relatively short timescale. In general, however, we are able to confirm the predictions of Ref. [14], namely that strongly self interacting dark matter produces halos with shallower density profiles and thus can remedy the problems that the standard cold dark matter model has in explaining galactic dynamics. It should be noted here that self interacting dark matter has been considered previously, in order to study possible effects on the initial linear power spectrum [15–17]. However, the type of self interactions investigated in the present paper will have no discernible effects on the initial power spectrum.

II. THE PHYSICS OF SELF-INTERACTING DARK MATTER

In the standard cold dark matter model, the dark matter particles were once in thermal equilibrium in the early universe. As the temperature dropped below their rest mass, however, their abundance was exponentially suppressed. Eventually annihilation reactions were no longer

effective and the abundance of dark matter particles froze out at some particular value [18]. In this picture, the dark matter particles are presently extremely weakly interacting and halos consisting of them behave as collisionless systems. However, dark matter particles could in principle have very strong self-interaction, as long as their reaction cross section with standard model particles is small. That is for instance the case with the non-thermally produced particles proposed by Chung, Kolb and Riotto [19]. In the present paper we shall assume only that dark matter particles are completely decoupled from all other species. The dark matter self-interactions are modelled as point-like, i.e. the interactions are mediated by some very massive boson. In that case, the cross section for two-body scattering, σ , is energy-independent. This means that the reaction rate for a dark matter particle moving in a dark matter halo is

$$\Gamma = \int \frac{d^3p}{(2\pi)^3} f_p v_{\text{rel}} \sigma, \quad (1)$$

where v_{rel} is the relative velocity between the incident particle and the target and f_p is the phase-space distribution of dark matter particles. As will be explained later, the cross-section that divides the very weakly interacting regime from the strongly interacting one is given roughly by

$$\sigma_0 \simeq 1 \times 10^{-22} \text{ cm}^2 m_{\text{GeV}}^{-1}, \quad (2)$$

which of course is many orders of magnitude larger than the interaction cross section for standard cold dark matter.

III. NUMERICAL SCHEME

The fundamental equation describing the phase-space evolution of self-interacting dark matter is the Boltzmann equation. We shall in the present paper neglect the Hubble expansion of the universe. In that case, the Boltzmann equation takes on the form

$$\frac{df}{dt} = \frac{\partial f}{\partial t} + \mathbf{v} \cdot \frac{\partial f}{\partial \mathbf{r}} + \mathbf{a} \cdot \frac{\partial f}{\partial \mathbf{v}} = C[f], \quad (3)$$

where the right-hand side is a collision operator describing possible scattering/annihilation reactions.

For normal, collisionless matter, the right hand side is zero, but in our case it is a phase space integral of the reaction matrix element.

In order to keep the numerical work quite simple, while still retrieving the essential physics, we shall assume spherical symmetry of f . In that case, there are only four independent phase space coordinates, (t, r, v_r, v_\perp) . Instead of v_\perp we use the specific angular momentum, $j \equiv v_\perp r$, which is a conserved quantity for collisionless systems [20]. The left hand side of the Boltzmann equation is then [20]

$$\frac{df}{dt} = \frac{\partial f}{\partial t} + v_r \frac{\partial f}{\partial r} + \left(\frac{j^2}{r^3} - \frac{GM(r)}{r^2} \right) \frac{\partial f}{\partial v_r}. \quad (4)$$

Our numerical scheme for solving the Boltzmann equation is somewhat similar to that of Rasio, Shapiro and Teukolsky [21]. We mimic the phase space distribution by particles, distributed according to the initial f . Then these particles are moved in phase-space according to the Boltzmann equation. Thus, the force on each phase-space ‘‘particle’’ is calculated using the mean gravitational field produced by all particles, $GM(r)/r$. All mean field quantities, like $M(r)$, are calculated on an Eulerian grid in phase-space and interpolated using spline interpolation. Thus, the code is a hybrid between a real Boltzmann code and an N-body code. This is a standard way of solving the collisionless Boltzmann equation, both in gravitational dynamics and in plasma physics [22,23].

The right-hand side depends on the specific scattering process. In the case of two-body scattering, it can be written as [18]

$$C[f] = \frac{1}{2E} \int d^3\tilde{p}_2 d^3\tilde{p}_3 d^3\tilde{p}_4 \Lambda(f, f_2, f_3, f_4) \times \sum |M_{12 \rightarrow 34}^2| \delta^4(p_1 + p_2 - p_3 - p_4) (2\pi)^4. \quad (5)$$

Here we have used the definition $d^3\tilde{p} \equiv d^3p / ((2\pi)^3 2E)$. $\sum |M|^2$ is the interaction matrix element and p_i is the four-momentum of particle i . The phase-space factor is defined as $\Lambda \equiv f_3 f_4 (1-f)(1-f_2) - f f_2 (1-f_3)(1-f_4)$.

However, since we are considering phase space to be sampled by a distribution of particles, changing the phase space density due to collisions amounts to letting the particles scatter on each other.

The interaction rate for a given particle can therefore be written as in Eq. (1)

$$\Gamma = \int \frac{d^3p}{(2\pi)^3} f_p v_{\text{rel}} \sigma \simeq n \sigma v_{\text{disp}}, \quad (6)$$

where v_{disp} is the velocity dispersion of the system. Therefore, in this simple approximation, the interaction rate of a dark matter particle is given in terms of the simple mean field quantities n and v_{disp} .

The above system of equations can be relatively easily solved for given initial conditions, and quantities such as the radial density distribution and velocity dispersion can be recovered.

IV. RESULTS

We have solved the system of equations described in the previous section for different values of the interaction cross section, σ . The Boltzmann equation is non-dimensionalised in the following way: Given a total mass M_0 of the system and a characteristic radius R_0 , the system is non-dimensionalised by solving in terms of the dynamical time $\tau = \sqrt{R_0^3 / GM_0}$ and the characteristic

velocity $v_0 = \sqrt{GM_0/R_0}$. The interaction cross section should then be cast in units of $\sigma_0 = mR_0^2/M_0$, where m is the mass of the dark matter particle. Note that for $\sigma = \sigma_0$, the mean free path in a typical system should be $\lambda \simeq R_0$, so that that σ_0 is a natural dividing line between slow and fast interactions.

In all the simulations we start with a homogeneous sphere of radius R_0 . The velocity dispersion is assumed to be Maxwellian so that

$$f \propto \exp(-v_r^2/2v_d^2 - j^2/2r^2v_d^2). \quad (7)$$

The velocity dispersion, v_d , is chosen to be $v_d = 0.1v_0$. If all particles start at rest, they will pass through the center at the same time, and the simulation becomes unstable [24]. However, letting the particles have a small initial velocity does not alter the final state of the whole system very much. It only results in the collisionless systems being slightly less centrally concentrated.

The system is allowed to evolve until $t = 30\tau$, in order to test stability of the code.

A. Collisionless systems

The first simulation was done for a normal collisionless dark matter halo. Fig. 1 shows how the mass distribution $M(r)$ evolves with time. As expected, the system very quickly approaches equilibrium, essentially in just one dynamical time. The core profile of the relaxed system approximately follows a power law, $\rho \propto r^{-4/3}$. Note that if the initial velocity of all particles was zero, the final system would have a density profile with $\rho \propto r^{-9/8}$ instead [24]. Thus, our assumption of a small initial velocity leads to a less centrally concentrated halo structure. However, since our purpose is to compare halos of dark matter with different interaction strengths, and not so much to make exact calculations, this assumption does not matter much.

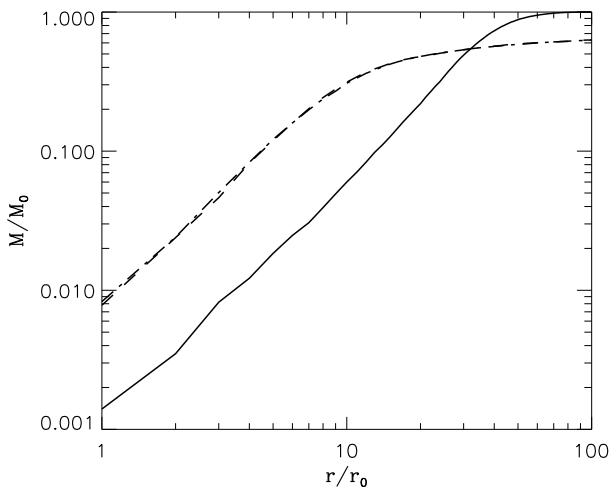


FIG. 1. The mass distribution, $M(r)$, for the collisionless dark matter collapse at three different times. The solid line is for $t = \tau$, the dashed for $t = 10\tau$, and the dot-dashed for $t = 20\tau$.

B. Collisional systems

Ejection — As described above, $\sigma = \sigma_0$ divides the weakly and strongly interacting regimes. For $\sigma \ll \sigma_0$, one would expect an evolution very similar to the fully collisionless system, whereas for $\sigma \gg \sigma_0$, the system will behave like a collisional gas, i.e. shocks can be produced and single particles will perform random walks in phase space. The halo should therefore behave like an entirely hydrodynamical core surrounded by a collisionless system. However, at $\sigma \simeq \sigma_0$ the evolution is less obvious. As also noted in Ref. [14], most self gravitating systems can eject particles. In normal collisionless systems, this can happen for two reasons, either a particle experiences a single close encounter which leaves it with positive energy [25] or it suffers many weak collisions, gradually increasing its energy [26]. The first process is usually referred to as ejection, whereas the second is called evaporation. This process makes the entire system unstable in the long term, since the only stable solution is a single pair of particles in a Kepler orbit, with all other particles being at infinity [27]. However, for a normal galaxy of stellar objects, the instability time is vastly larger than the Hubble time, and for a collisionless dark matter halo it is for all practical purposes infinite.

However, for a collisional halo, this need not be the case. Since particle interactions are point-like, a given particle can normally only gain positive energy because of a single scattering event, not because of many weak collisions. We can estimate the instability time in the following way: In a homogeneous mass distribution with a typical velocity $v_0 = \sqrt{GM_0/R_0}$, a particle passing through the entire system has the scattering probability

$$P \simeq 1 - e^{-R_0/\lambda}, \quad (8)$$

where

$$\lambda \simeq \frac{mc}{\sigma \sqrt{\rho_0^3 R_0^2 G}}. \quad (9)$$

If the particle scatters, and acquires a positive energy, then it should not scatter again on its way out, if it is to be ejected. Therefore the total probability for the particle to be ejected is roughly

$$P_{\text{ejection}} \simeq (1 - e^{-R_0/\lambda})e^{-R_0/\lambda}P(E_{\text{final}} > 0). \quad (10)$$

$P(E_{\text{final}} > 0)$ is the probability that the energy after scattering is larger than zero. Normally this probability will be $P(E_{\text{final}} > 0) \simeq 0.1 - 0.2$, so that it is not negligible. The probability is maximal when $\lambda \simeq R_0$, as could be expected. The typical timescale for instability is then roughly

$$t_{\text{instability}} \simeq \tau/P_{\text{ejection}}, \quad (11)$$

From these extremely crude estimates one finds that the minimal possible instability time of of the order $t_{\text{instability}} \simeq \text{few} \times \tau$. Even if interactions are very strong, the system is unstable in the long term, because particle will escape from the system via diffusion [14]. However, the timescale for this diffusion process is much longer than the Hubble time.

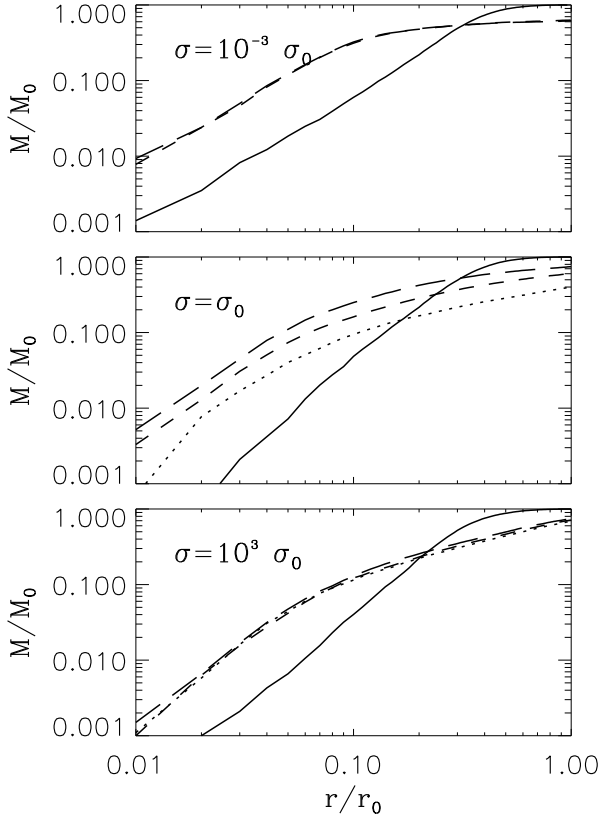


FIG. 2. The mass distribution as a function of r at three different times and three different values of σ . The solid lines are for $t = \tau$, the long-dashed for $t = 15\tau$, the dashed for $t = 20\tau$ and the dotted for $t = 25\tau$.

Numerical simulations — We have performed simulations for different values of σ/σ_0 , specifically $\sigma/\sigma_0 = 10^{-3}, 10^{-2}, 10^{-1}, 1, 10, 100, 1000$. Fig. 2 shows the evolution of $M(r)$ for $\sigma/\sigma_0 = 10^{-3}, 1$ and 10^3 . For $\sigma/\sigma_0 = 10^{-3}$, it is practically indistinguishable from the collisionless case, as would be expected. For the very strongly interacting case $\sigma/\sigma_0 = 1000$, we find a very different behaviour. The system again settles into equilibrium very fast, roughly at $t \simeq \text{few} \times \tau$, but we also see that the core is much less dense because low entropy material is ejected. This is the result predicted by Ref. [14].

The intermediate case, $\sigma/\sigma_0 = 1$, never settles into a true long-term equilibrium. It starts out by approaching the collisionless equilibrium, but scattering interaction

drives the mass distribution towards the equilibrium distribution for the strongly interacting particles. However, on the same timescale the system loses particles due to the ejection mechanism described above, so that no true equilibrium is ever reached. The timescale for particle loss indeed seems to be $\sim 10 \times \tau$.

Observations — We cannot expect our simulations to fit observational rotation curves because of the approximations we have made, i.e. Hubble expansion was neglected and spherical symmetry was assumed. Nevertheless, it is interesting to compare our results to observations. In Fig. 3 we show the predicted rotation curves at $t = 15\tau$ for the three different values, $\sigma = 10^{-3}, 1$ and 10^3 . The rotation curve for the strongly interacting halo is much less centrally peaked than the collisionless one.

The crosses in Fig. 3 show the measured rotation curve for the typical low surface brightness galaxy UGC128 [9]. The observational curve has an asymptotic circular rotation velocity of $v = 200$ km/s at $R = 100$ kpc. Taking $v_0 = 200$ km/s and $R_0 = 100$ kpc gives a mass of $M_0 = 1.35 \times 10^{12} M_\odot$ and a dynamical timescale of $\tau = 4.7 \times 10^8$ y. These numbers are typical for such galaxies. Notice that for this choice of mass and radius, $\sigma_0 = 8.5 \times 10^{-23} \text{cm}^2 m_{\text{GeV}}^{-1}$, i.e. corresponding to the σ_0 quoted in Eq. (2).

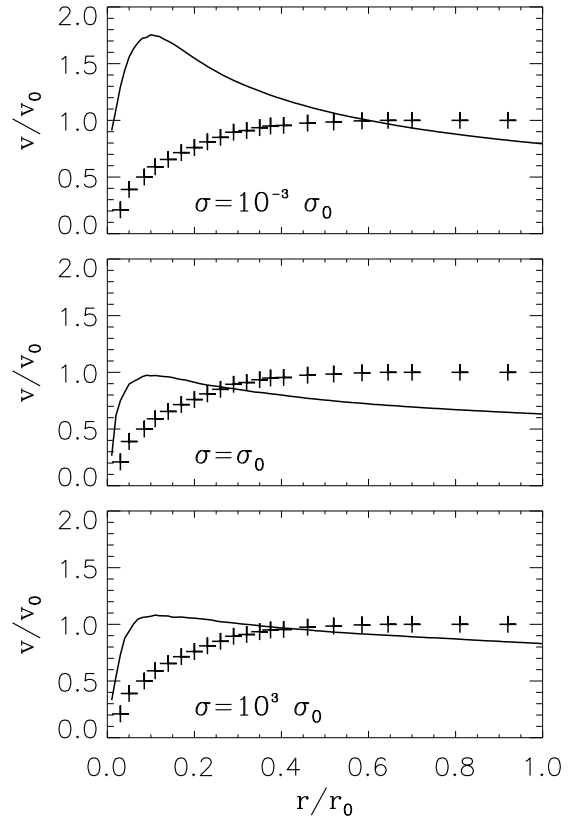


FIG. 3. The rotational velocity at $t = 20\tau$ for three different values of σ . The crosses are the observational rotation curve for the low surface brightness galaxy UGC128 [9].

The rotation curve for the strongly interacting system provides a better fit to the observational rotation curve than that for the collisionless system. However, in all cases, the fits are quite poor. As mentioned, this should not be taken too seriously since our model involves some essential approximations.

V. DISCUSSION

We have performed quantitative calculations of how dark matter halos form in models with self interacting dark matter. For simplicity we assumed spherical symmetry, neglected the Hubble expansion, and used a very simple prescription for the dark matter self-interaction.

Our results have essentially confirmed the estimates of Ref. [14], in that dark matter halos with sufficient self interaction will have much shallower density profiles than normal collisionless halos. Thus, they can provide better fits to observational galactic rotation curves, while still being consistent with all other known data.

A very curious feature is that halos with intermediate self interaction ($\lambda \simeq R_0$) are unstable on a rather short timescale because they eject particles continuously. This effect was estimated to be unimportant in Ref. [14], but our numerical simulations indicate that there exist regions of parameter space where the instability would probably have shown up in present day halos.

As mentioned, our calculations assume spherical symmetry and neglect the Hubble expansion. It will be very interesting to investigate the effect of self interacting dark matter using detailed N-body calculations [28]. Most likely, such simulations will confirm the general statements made by Spiegel and Steinhardt [14] as well as in the present paper.

ACKNOWLEDGMENTS

Support from the Carlsberg foundation is gratefully acknowledged.

[8] J. F. Navarro and M. Steinmetz, astro-ph/9908114 (1999).
 [9] B. Moore *et al.*, astro-ph/9903164 (1999).
 [10] J. F. Navarro, C. S. Frenk and S. D. M. White, *Astrophys. J.* **462**, 563 (1996).
 [11] A. V. Kravtsov *et al.*, *Astrophys. J.* **502**, 48 (1998).
 [12] R. Schaefer and J. Silk, *Astrophys. J.* **332**, 1 (1988).
 [13] M. Kamionkowski and A. R. Liddle, astro-ph/9911103 (1999).
 [14] D. N. Spergel and P. J. Steinhardt, astro-ph/9909386 (1999).
 [15] E. D. Carlson, M. E. Machanek and L. J. Hall, *Astrophys. J.* **398**, 43 (1992).
 [16] A. de Laix, R. J. Scherrer and R. K. Schaefer, *Astrophys. J.* **452**, 495 (1995).
 [17] F. Atrio-Barandela and S. Davidson, *Phys. Rev. D* **55**, 5886 (1997).
 [18] E. W. Kolb and M. S. Turner, *The Early Universe*, Addison Wesley (1990).
 [19] D. Chung, E. Kolb and A. Riotto, *Phys. Rev. Lett.* **81**, 4048 (1998).
 [20] T. Fujiwara, *Publ. Astron. Soc. Japan* **35**, 547 (1983).
 [21] F. A. Rasio, S. L. Shapiro and S. A. Teukolsky, *Astrophys. J.* **344**, 146 (1989).
 [22] J. A. Selwood, *Ann. Rev. Astron. Astrophys.* **25**, 151 (1987).
 [23] R. W. Hockney and J. W. Eastwood, *Computer Simulation Using Particles*, McGraw-Hill (1981).
 [24] E. Bertschinger, *Astrophys. J. Suppl.* **58**, 39 (1985).
 [25] M. Henon, *Astron. Astrophys.* **2**, 151 (1969).
 [26] M. Henon, *Ann. Astr.* **23**, 668 (1960).
 [27] J. Binney and S. Tremaine, *Galactic Dynamics*, Princeton Series in Astrophysics, Princeton University Press (1987).
 [28] T. K. Nielsen and S. Hannestad, in preparation (2000).

[1] F. Zwicky, *Helvetica Physica Acta* **6**, 110 (1933).
 [2] See for instance M. Gross *et al.*, *Mon. Not. R. Astron. Soc.* **301**, 81 (1998).
 [3] B. Moore *et al.*, astro-ph/9907411 (1999).
 [4] S. Ghigna *et al.*, astro-ph/9910166 (1999).
 [5] J. Tyson, G. Kochanski and I. P. Dell'Antonio, *Astrophys. J. Lett.* **498**, L107 (1998).
 [6] R. Flores and J. R. Primack, *Astrophys. J.* **427**, L1 (1994).
 [7] J. F. Navarro, astro-ph/9807084 (1998).